

Enhanced Monte Carlo Simulation of the Voxel Phantom Lattice Submersed in a Contaminated Air Environment

American Nuclear Society
Annual Meeting
June 13, 2017

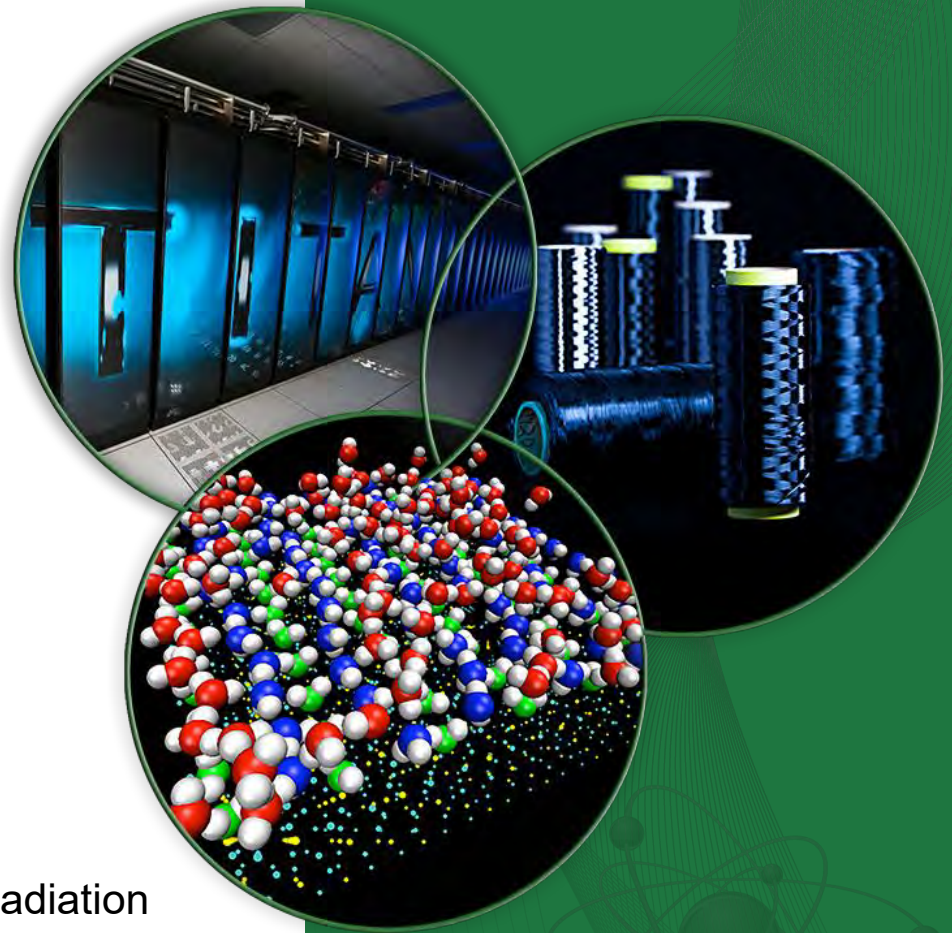
K.G. Veinot^{1,2}, **S.A. Dewji**^{3*},
M.M. Hiller³, **K.F. Eckerman**¹,
C.E. Easterly¹

¹Easterly Scientific

²Y-12 National Security Complex

³Oak Ridge National Laboratory, Center for Radiation
Protection Knowledge

<https://ornl.gov/crpk>
crpk@ornl.gov



Center for Radiation Protection Knowledge (<https://ornl.gov/crpk/>)

- Established at ORNL per MOU 2010
 - DOE, DoD, EPA, NRC, and OSHA
- MOU Renewal in 2015



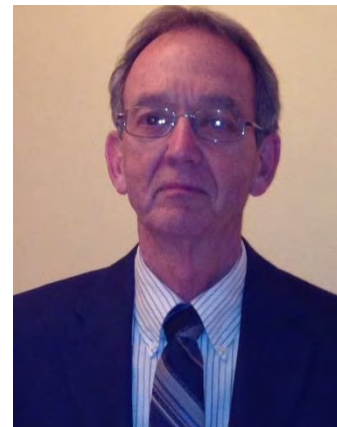
- Objectives
 - Maintaining/Preserving U.S. expertise and leadership
 - Development/Application of Radiation Dosimetry and Risk Assessment Methodologies/Models
 - Ensure the best scientifically available knowledge in regulatory processes and decision making

Center for Radiation Protection Knowledge

<https://ornl.gov/crpk>

Top:

Nolan Hertel (JFA, Georgia Institute of Technology)
Keith Eckerman (Emeritus)
Rich Leggett (Senior R&D Scientist)



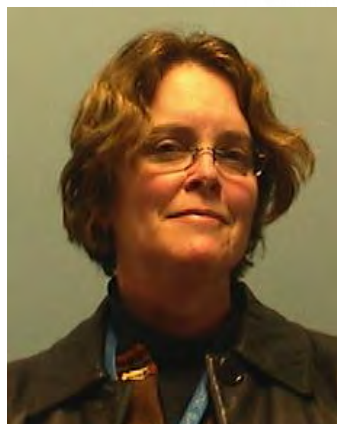
Middle:

Michael Bellamy (ORNL, R&D Engineer)
Shaheen Dewji (ORNL, R&D Engineer)
Derek Jokisch (JFA, Francis Marion U)



Bottom:

Clay Easterly (Consultant)
Ken Veinot (Consultant)
Pat Scofield (ORNL)
Scott Schwahn (ORNL)



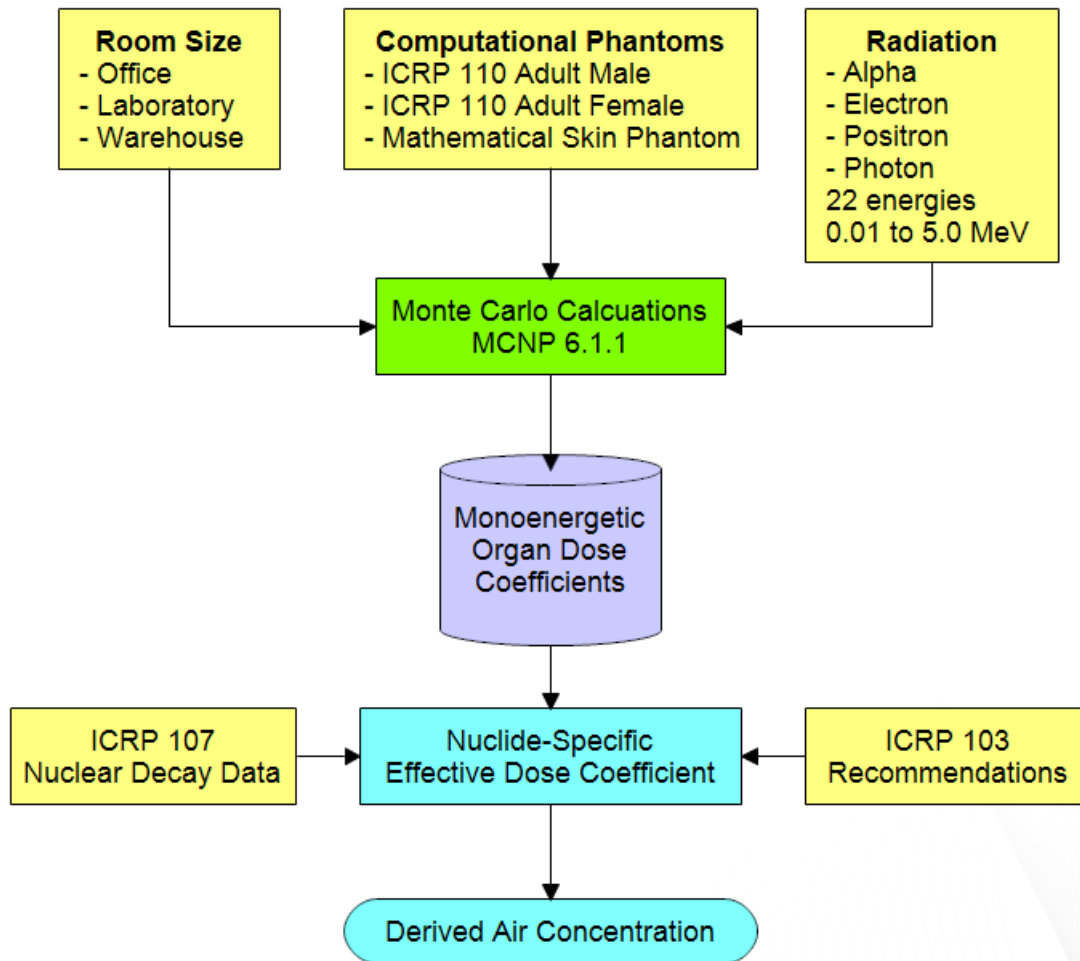
Alumnus:

Mauritius Hiller

Introduction

- ICRP Publication 30 contained dosimetric data for occupational external exposure to noble gas radionuclides which has not been updated.
- In this work, voxel phantoms positioned in three rooms of finite sizes representing
 - office, laboratory, and warehouse
 - dose coefficients computed for monoenergetic alpha, photons, electrons, and positrons.
- Monoenergetic response coefficients used to derive nuclide specific **effective dose coefficient** and their **derived air concentrations**.
 - emission data of ICRP 107
 - tissue weighting factor of ICRP 103

Methodology



Calculation of derived air concentration for noble gases.

Methodology – Monte Carlo Simulation

Table 1: Room dimensions and geometry.

Room	Dimensions (m)	Volume (m ³)	Composition (cm)
Small (Office)	5.8 × 5.8 × 3.0	100.92	Walls and Ceiling: <ul style="list-style-type: none">• 2.54 cm (1-inch) concrete• 1.27 cm (½-inch) sheet rock Floor: <ul style="list-style-type: none">• 30 cm concrete
Medium (Laboratory)	10 × 20 × 30	600	Walls and Ceiling: <ul style="list-style-type: none">• 2.54 cm (1-inch) concrete• 1.27 cm (½-inch) sheet rock Floor: <ul style="list-style-type: none">• 30 cm concrete
Large (Warehouse)	15 × 15 × 5.3	1192	Walls and Ceiling: <ul style="list-style-type: none">• 20.32 cm (8-inches) concrete• No sheetrock Floor: <ul style="list-style-type: none">• 30 cm concrete

ICRP 110 Reference Computational Phantoms



Characteristics of adult male and female reference computational phantoms		
Property	Male	Female
Height (m)	1.76	1.63
Mass (kg)	73.0	60.0
Voxel dimension: Z-direction (mm) ⁽¹⁾	8.0	4.84
Voxel dimension: X- & Y-direction (mm)	2.137	1.775
Voxel volume (mm ³)	36.54	15.25
Number voxels along X-axis	254	299
Number voxels along Y-axis	127	137
Number of voxels along Z-axis	222	348
Number tissue voxels	1,950,255	3,887,730
Number of void voxels	5,211,021	10,367,394
Total number of voxels	7,161,276	14,255,124

(1) Axis orientation: X-axis right to left; Y-axis front to back, Z-axis feet to head.

Methodology – Monte Carlo Simulation

- Calculations performed in each room type for four radiation types, three phantoms with source in both the room and void voxels of the two voxel phantoms.
 - Non-tissue voxels surrounding phantom in the voxel lattice require separate source simulation
 - Two-phase approach was required to simulate the voxel phantoms in the non-tissue voxels in the lattice
 - (1) Source radiation in room air (external to voxel phantom lattice)
 - (2) Source radiation in non-tissue voxels of the voxel phantom lattice

Methodology – Monte Carlo Simulation

(1) Source radiation in room air
external to voxel phantom lattice
(ROOM)

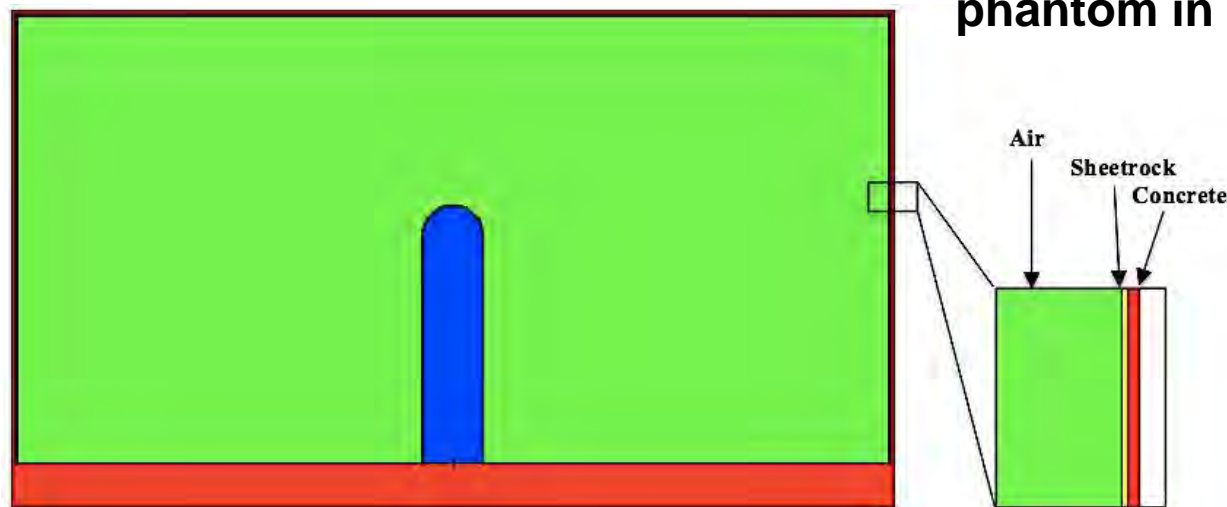


(2) Source radiation in
non-tissue voxels of the
voxel phantom lattice
(LATTICE/BOX)

Methodology – Monte Carlo Simulation (Skin)

- Voxel phantoms lack resolution to represent the skin cells at risk (50 – 90 μm depth). Skin dose coefficients based on a mathematical phantom.
- Male lens of eye coefficients are those of the reference adult female phantom (male voxel phantom lacks sufficient resolution).

Depiction of mathematical phantom in the office setting.



Effective dose rate coefficient, \dot{e}

The effective dose rate coefficient \dot{e} is given by

$$\dot{e} = \sum_T w_T \left[\frac{\dot{h}_{T,M} + \dot{h}_{T,F}}{2} \right]$$

where w_T is the tissue weighting factor specified in ICRP 107 for tissue T . $\dot{h}_{T,M}$ and $\dot{h}_{T,F}$ are the equivalent dose rate coefficients for tissue T of the adult male and adult female, respectively.

ICRP Publication 103 Tissue Weighting Factors

Tissue	w_T
Bone marrow, breast, colon, lung, stomach and remainder tissues*	0.12
Gonads	0.08
Urinary bladder, esophagus, liver and thyroid	0.04
Bone surface, brain, salivary glands and skin	0.01

*Remainder tissues: adrenals, extrathoracic airways, gall bladder, heart, kidneys, lymphatic nodes, muscle, oral mucosa, pancreas, prostate (male), small intestine, spleen, thymus and uterus/cervix (female).

Nuclide-specific dose rate coefficient, \dot{h}_T

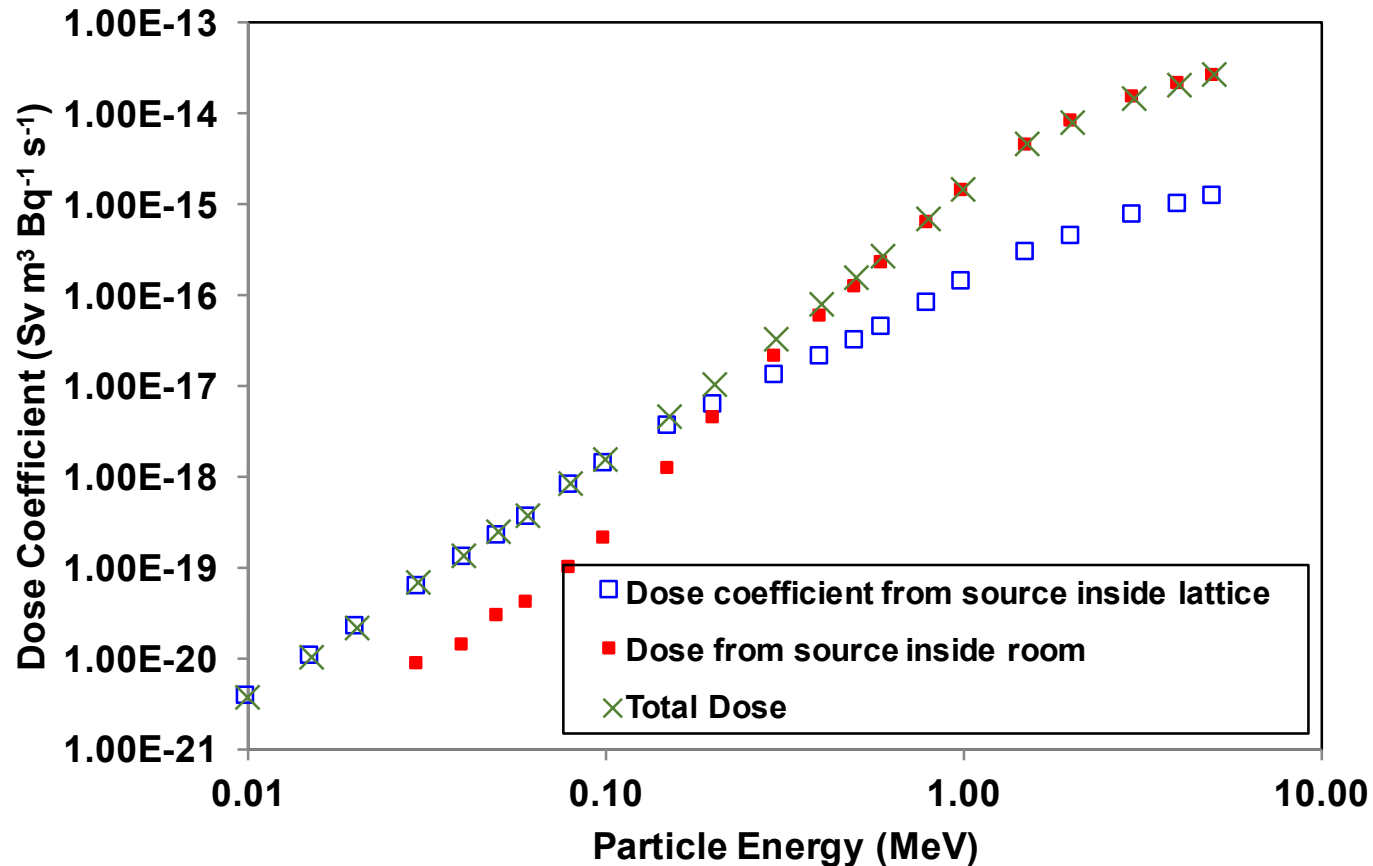
Dose rate coefficient, \dot{h}_T , for target tissue T

$$\dot{h}_T = \sum_i^n \sum_j^{n_i} Y_{i,j} E_{i,j} R_i(T, E_{i,j}) + \int_0^\infty N(E) E R_e(T, E) dE$$

where the summation of the first term extends over radiation type i (alpha, photon, and conversion electron) with its inner summation extending over the number of such emissions with energy $E_{i,j}$, yield $Y_{i,j}$ and monoenergetic response $R_i(T, E_{i,j})$. The second term integrates the response $R_e(T, E)$ over the beta spectra $N(E)$.

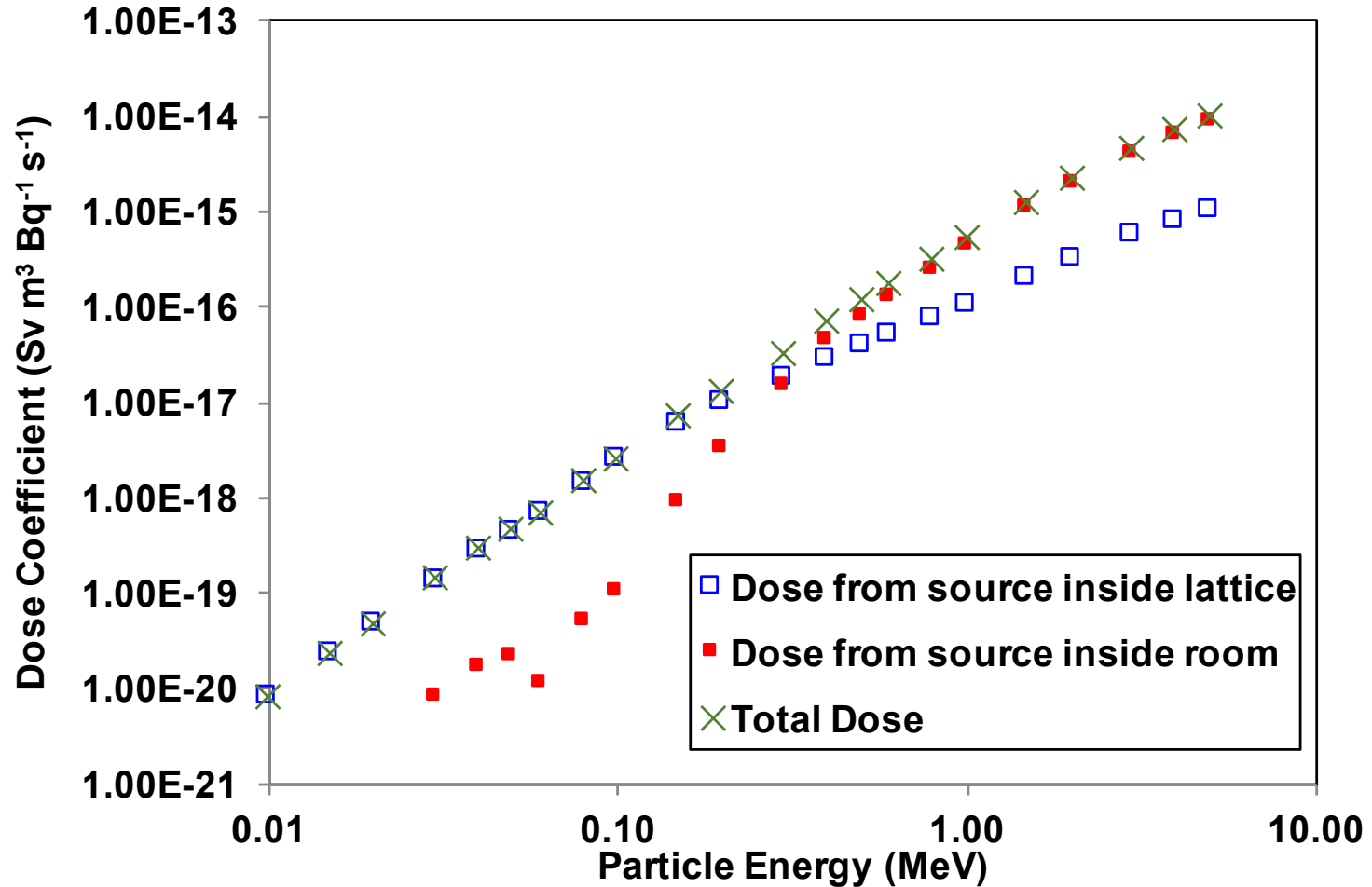
- The radiation emissions and beta spectra associated with the radionuclide are tabulated in ICRP Publication 107.

Results – Breast Dose Coefficient (Electron)



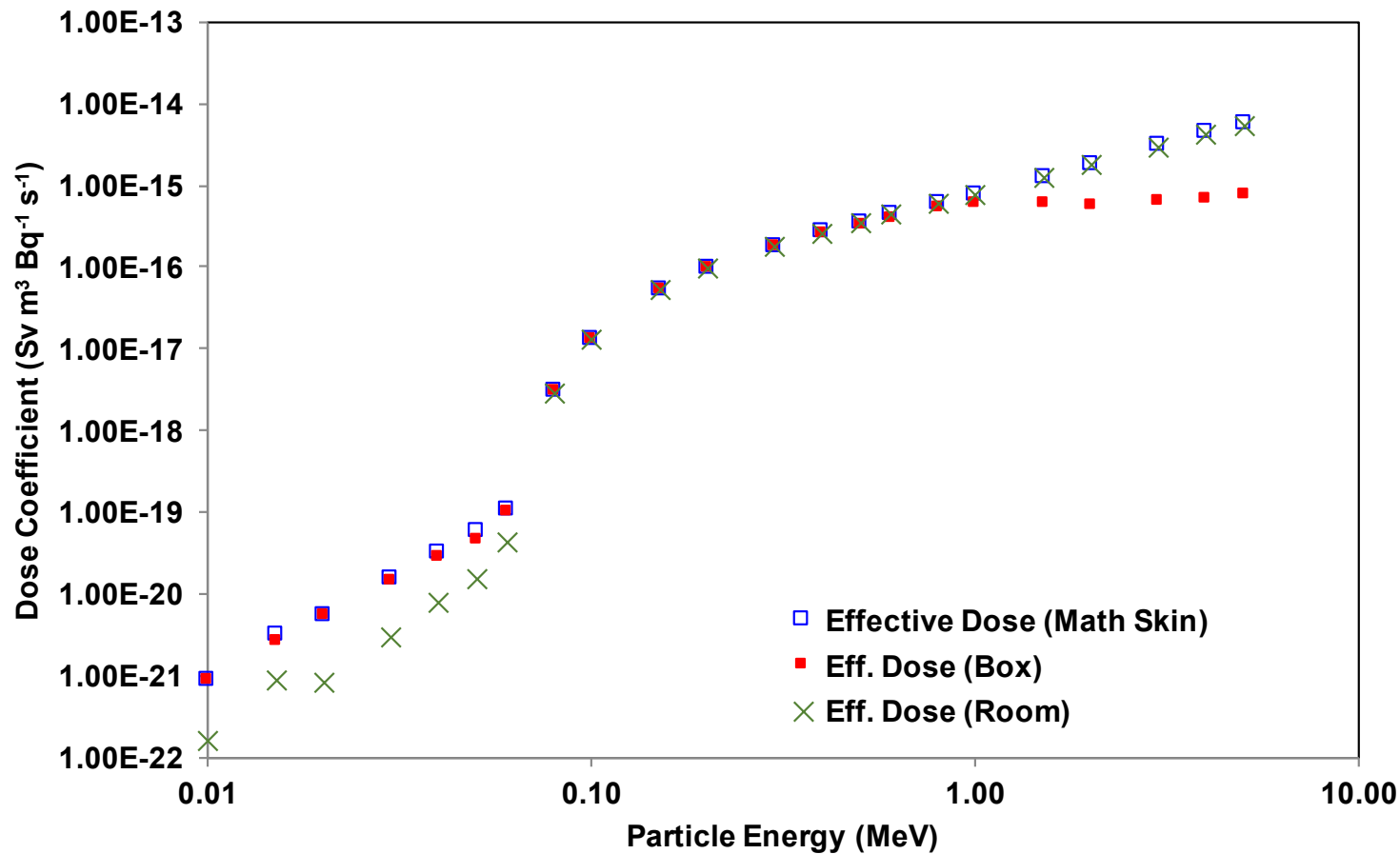
Female monoenergetic breast dose coefficients as a function of electron energy for voxel phantom lattice source, office room source, and combined total.

Results – Testes Dose Coefficient (Electron)



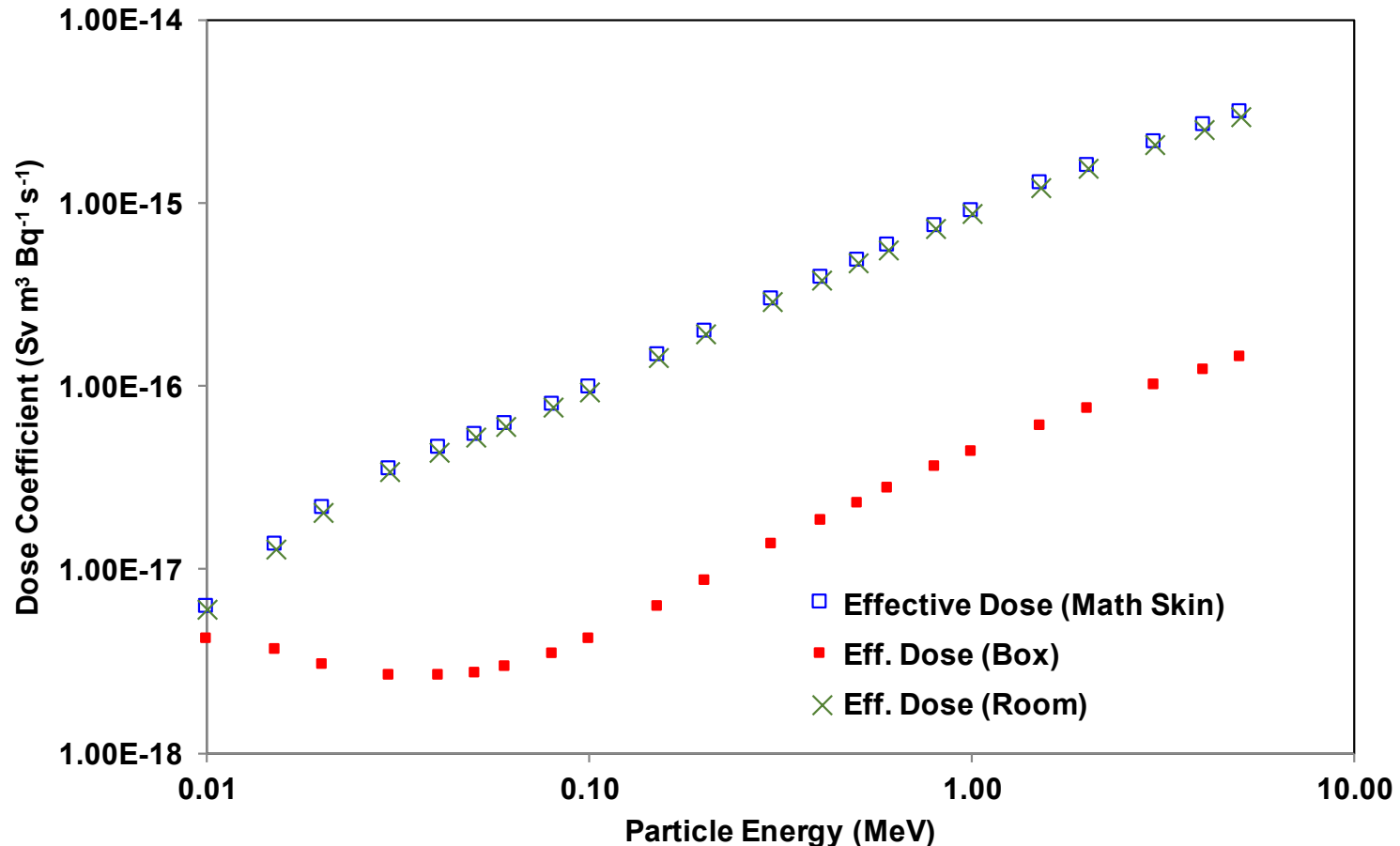
Male monoenergetic testes dose coefficients as a function of electron energy for voxel phantom lattice source, office room source, and combined total.

Results – Effective Dose Coefficient (Electron)



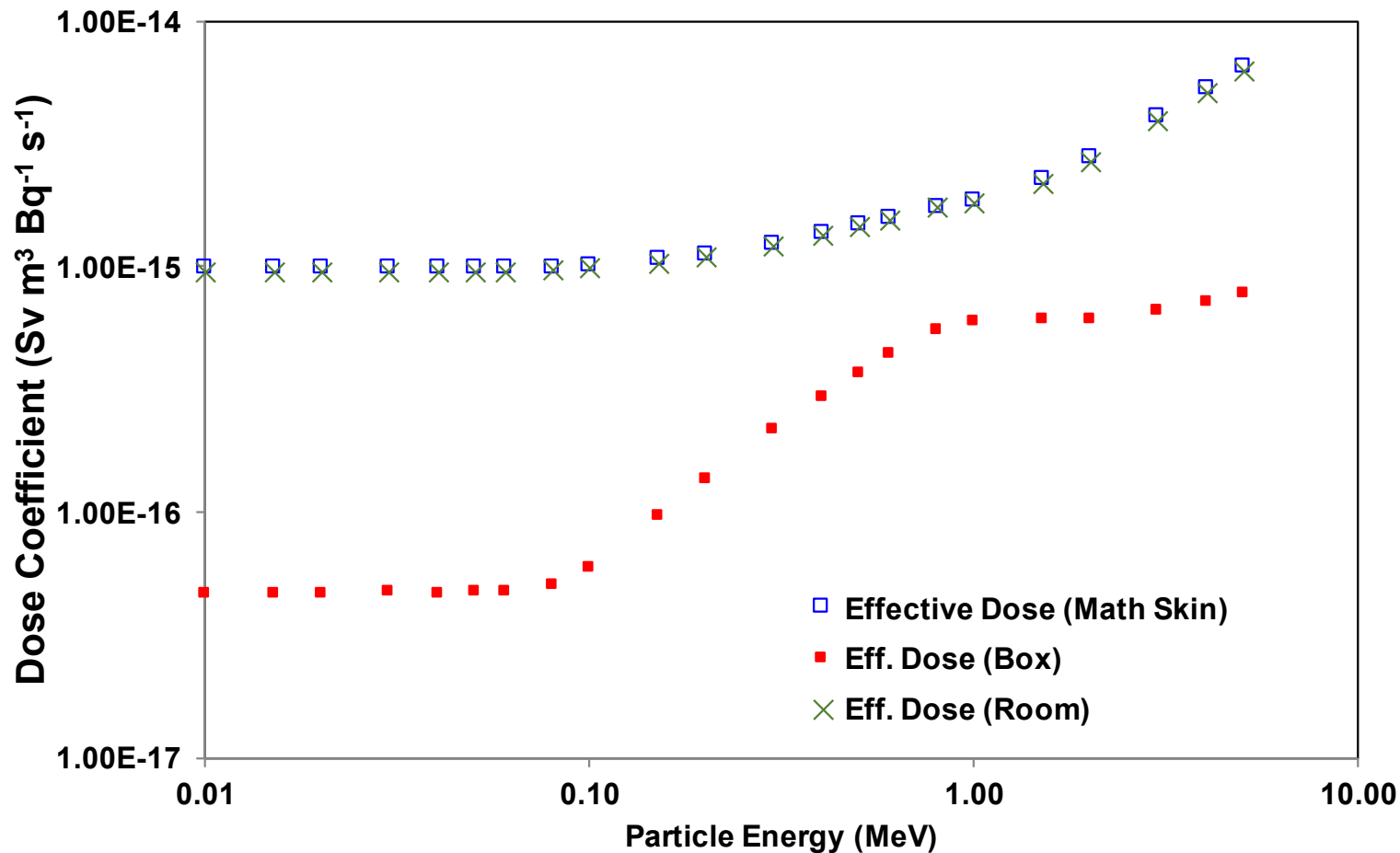
Effective dose coefficients for the office as a function of emitted electron energy.

Results – Effective Dose Coefficient (Photon)



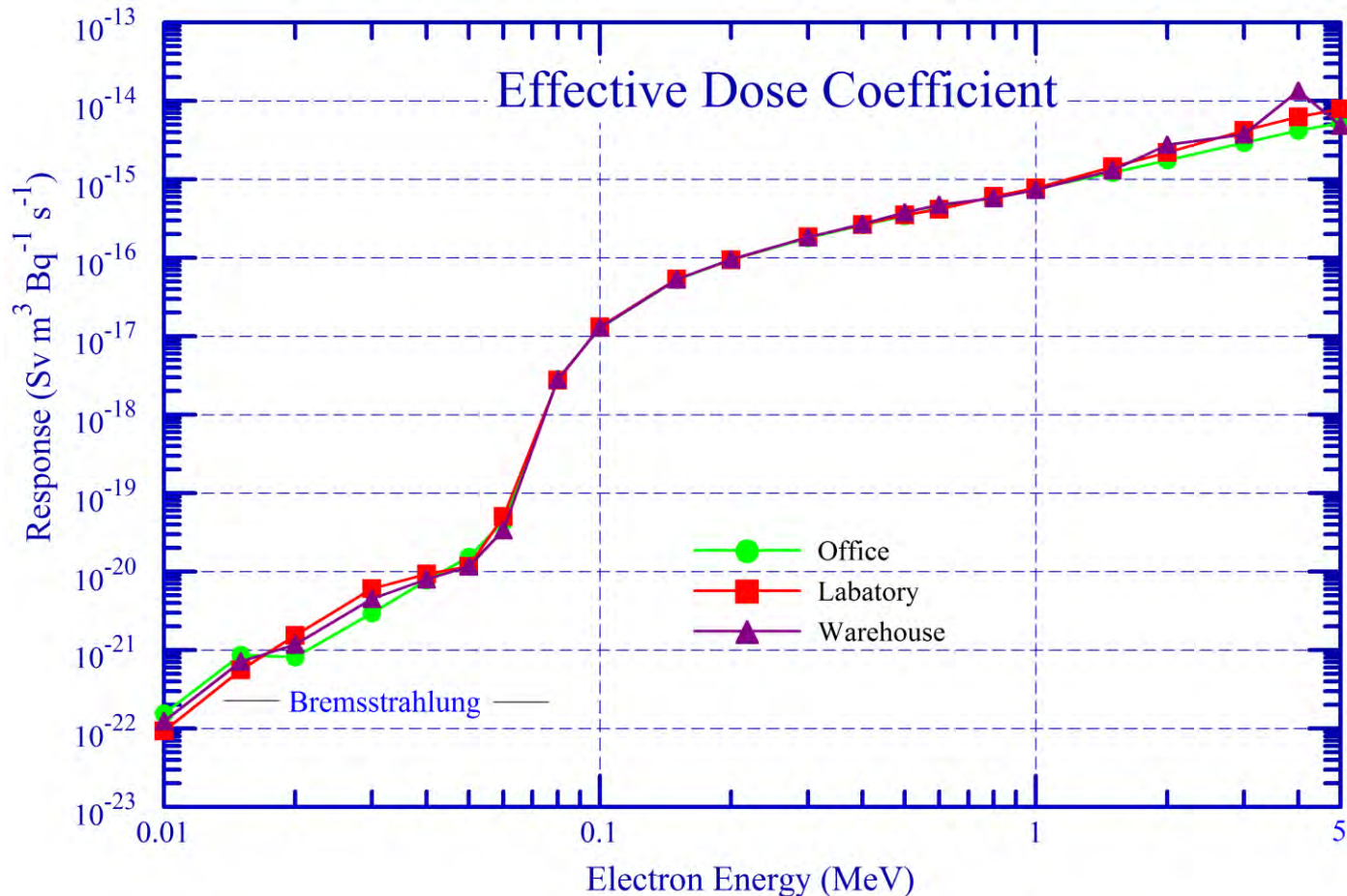
Effective dose coefficients for the office as a function of emitted photon energy.

Results – Effective Dose Coefficient (Positron)



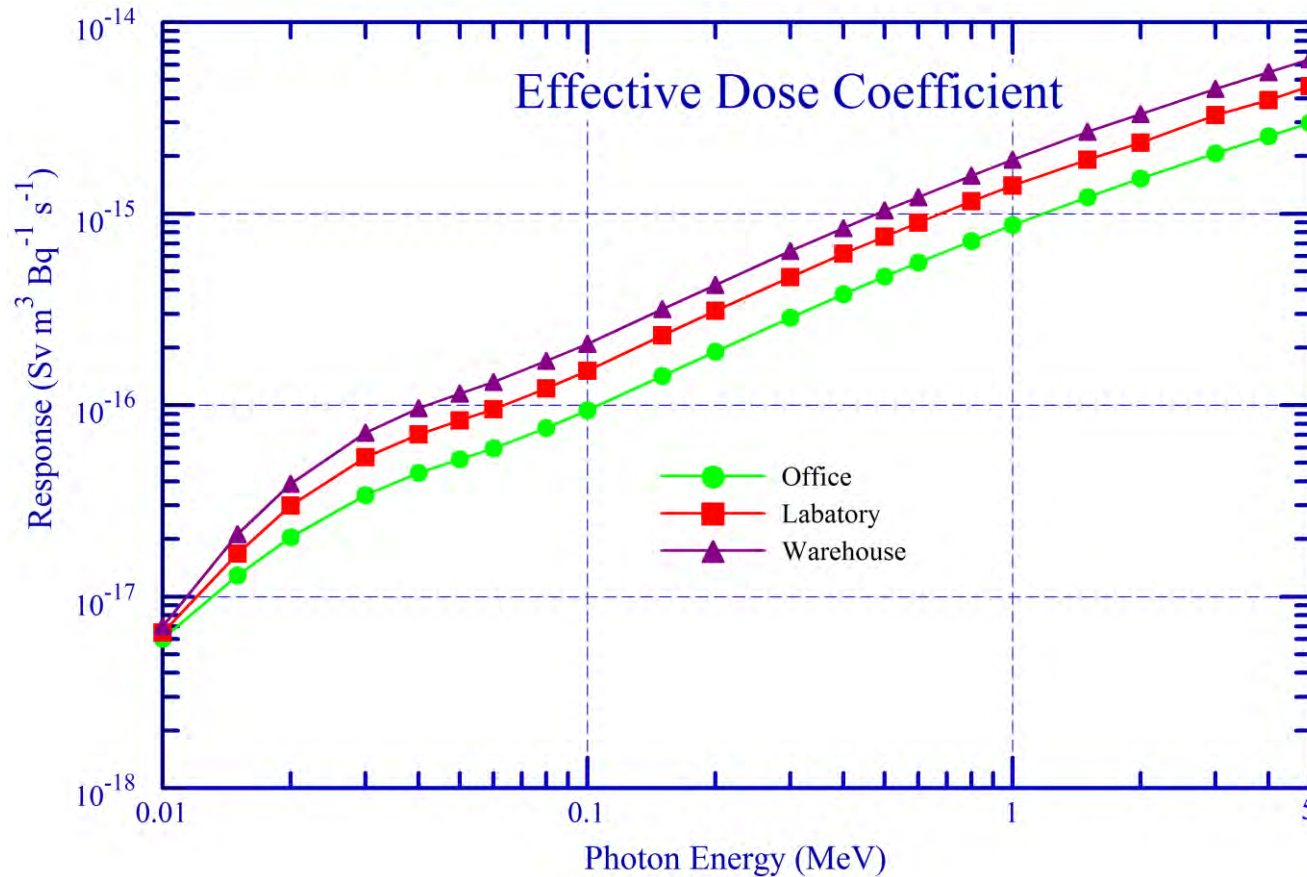
Effective dose coefficients for the office as a function of emitted positron energy.

Results – Room Effective dose (Electron)



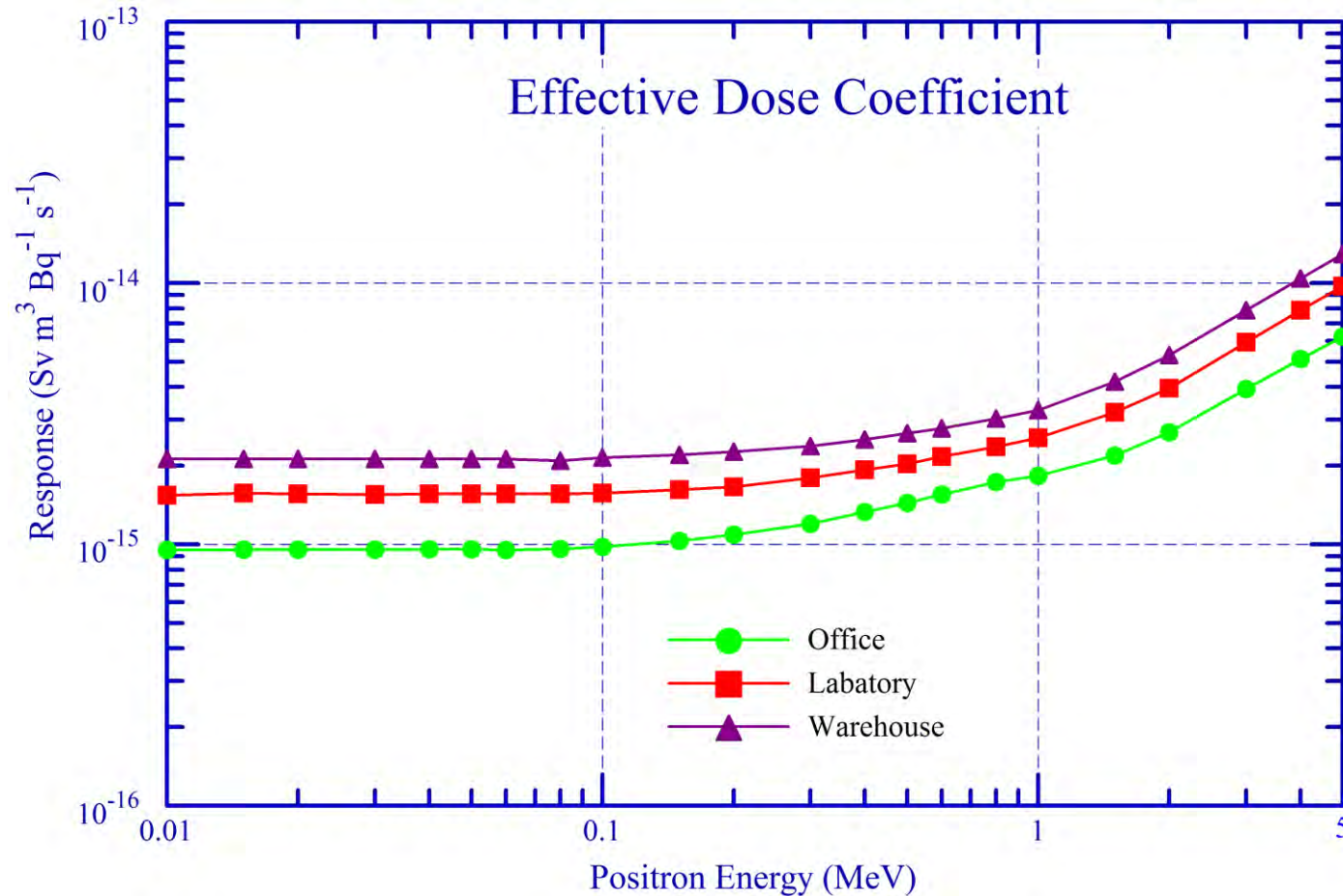
Effective dose coefficients for the office, laboratory and warehouse settings as a function of emitted electron energy.

Results – Room Effective dose (Photon)



Effective dose coefficients for the office, laboratory and warehouse settings as a function of emitted photon energy.

Results – Room Effective dose (Positron)



Effective dose coefficients for the office, laboratory and warehouse settings as a function of emitted positron energy.

Effective Dose Rate Coefficients

Effective Dose Coefficient for Submersion Exposure to Noble Gases			
Effective Dose Rate Coefficient (Sv m³ Bq⁻¹ s⁻¹)			
Nuclide	Office	Laboratory	Warehouse
Ar-39	1.17 x 10⁻¹⁶	1.19 x 10⁻¹⁶	1.21 x 10⁻¹⁶
Ar-41	1.39 x 10⁻¹⁵	2.02 x 10⁻¹⁶	2.69 x 10⁻¹⁵
Kr-83m	1.50 x 10⁻¹⁸	1.84 x 10⁻¹⁸	2.24 x 10⁻¹⁸
Kr-85	1.46 x 10⁻¹⁶	1.49 x 10⁻¹⁶	1.56 x 10⁻¹⁶
Kr-85m	2.87 x 10⁻¹⁶	3.82 x 10⁻¹⁶	4.78 x 10⁻¹⁶
Kr-88	1.76 x 10⁻¹⁵	2.64 x 10⁻¹⁵	3.57 x 10⁻¹⁵
Xe-131m	2.21 x 10⁻¹⁷	3.49 x 10⁻¹⁷	4.71 x 10⁻¹⁷
Xe-133	7.83 x 10⁻¹⁷	1.07 x 10⁻¹⁶	1.35 x 10⁻¹⁶
Xe-133m	4.16 x 10⁻¹⁷	6.68 x 10⁻¹⁷	9.08 x 10⁻¹⁷
Xe-135	4.24 x 10⁻¹⁶	5.75 x 10⁻¹⁶	7.25 x 10⁻¹⁶
Xe-135m	4.01 x 10⁻¹⁶	6.47 x 10⁻¹⁶	8.83 x 10⁻¹⁶
Xe-138	1.39 x 10⁻¹⁵	1.96 x 10⁻¹⁵	2.53 x 10⁻¹⁵

Derived Air Concentration, DAC

The derived air concentration (DAC) for a noble gas radionuclide is

$$DAC = \frac{E}{\dot{e} t}$$

where E is the ICRP Publication 103 recommended annual limit on effective dose (0.02 Sv), \dot{e} the radionuclide effective dose rate coefficient (Sv m³ Bq⁻¹ s⁻¹) and t is the annual occupational exposure time in seconds; i.e., 8 h daily, 50 weeks annually or 2000 h.

Results

- As the particle energies (and correspondingly their ranges) increase, the contributions from the room volume begins to dominate
- Effective dose coefficients for Ar-37 are zero.
 - Ar-37 decays by electron capture with Auger electrons of insufficient energy to penetrate skin dead layer.
- Effective dose coefficients for Ar-39/42 are dominated by the skin dose; *i.e.*, approximately the product of skin tissue weighting factor and its dose coefficient.
- Effective dose coefficient for nuclides decaying by positron emission dominated by the contribution of the annihilation radiation.
- For other radionuclides, the effective dose coefficients is due to the emitted photon and beta radiation with the latter resulting in bremsstrahlung.
- The DAC developed in this work are generally less restrictive than those of ICRP Publication 30 which often were limited by the 0.5 Sv restriction on the annual skin dose.

Results

Derived Air Concentration for Selected Noble Gases			
Nuclide	Derived Air Concentration (Bq m⁻³)*		
	Office	Laboratory	Warehouse
Ar-39	2 x 10⁷ (3.4)	2 x 10⁷ (3.3)	2 x 10⁷ (3.3)
Ar-41	2 x 10⁶ (1.0)	1 x 10⁶ (0.7)	1 x 10⁶ (0.5)
Kr-83m	2 x 10⁹ (2.1)	2 x 10⁹ (1.7)	1 x 10⁹ (1.4)
Kr-85	2 x 10⁷ (3.8)	2 x 10⁷ (3.7)	2 x 10⁷ (3.6)
Kr-85m	1 x 10⁷ (1.9)	7 x 10⁶ (1.5)	6 x 10⁶ (1.2)
Kr-88	2 x 10⁶ (0.8)	1 x 10⁶ (0.5)	8 x 10⁵ (0.3)
Xe-131m	1 x 10⁸ (6.3)	8 x 10⁷ (4.0)	6 x 10⁷ (3.0)
Xe-133	4 x 10⁷ (1.8)	3 x 10⁷ (1.3)	2 x 10⁷ (1.0)
Xe-133m	7 x 10⁷ (8.4)	4 x 10⁷ (5.2)	3 x 10⁷ (3.8)
Xe-135	7 x 10⁶ (1.6)	5 x 10⁶ (1.2)	4 x 10⁶ (1.0)
Xe-135m	7 x 10⁶ (0.7)	4 x 10⁶ (0.5)	3 x 10⁶ (0.5)
Xe-138	2 x 10⁶ (1.0)	1 x 10⁶ (0.5)	1 x 10⁶ (0.5)

***Value in parenthesis is the ratio this work to ICRP Publication 30.**

Conclusions

- Dose coefficients for three room sizes representing an office, laboratory, and warehouse were computed
 - Two-step approach was employed to simulate radiation in non-tissue voxels within the lattice surrounding the phantom
- Coefficients for electrons exhibit little dependence on room size for most energies
 - Organs within range of electron transport, dose from source activity within the non-tissue voxels of the lattice
 - Photon dose coefficients vary based on room size because of longer mean free paths
- Important to include the air surrounding the voxel phantom within the voxel lattice
 - Source particle energies below 200-300 keV
 - Else organ dose coefficient would be underestimated

References

- ICRP, 1979. *Limits for Intakes of Radionuclides by Workers*. ICRP Publication 30 (Part 1). Ann. ICRP 2 (3-4).
- Goorley, T., James, M., Booth, T., et al., 2012. Initial MCNP6 release overview. *Nuclear Technology*, 180(3), 298.
- ICRU, 1989. *Tissue Substitutes in Radiation Dosimetry and Measurement*, Report 44 of the International Commission on Radiation Units and Measurements (Bethesda, MD)
- ICRP, 2007. *The 2007 Recommendations of the International Commission on Radiological Protection*. ICRP Publication 103. Ann. ICRP 37 (2-4).
- ICRP, 2008. *Nuclear decay data for dosimetric calculations*. ICRP Publication 107. Ann. ICRP 38(3).
- ICRP, 2009. *Adult reference computational phantoms*. ICRP Publication 110. Ann. ICRP 39 (2).
- Nuclear Regulatory Commission, 2014. Title 10 Part 20, Appendix B, <http://www.nrc.gov/reading-rm/doc-collections/cfr/part020/part020-appb.html>
- McCoon Jr, R.J., C. J. Gesh, R.T. Pagh, R.A. Rucker, R.G. Williams, 2011. *Compendium of Material Composition Data for Radiation Transport Modeling*; PNNL-15870, Rev. 1.

Enhanced Monte Carlo Simulation of the Voxel Phantom Lattice Submersed in a Contaminated Air Environment

American Nuclear Society
Annual Meeting
June 13, 2017

**K.G. Veinot^{1,2}, S.A. Dewji^{3*},
M.M. Hiller³, K.F. Eckerman¹,
C.E. Easterly¹**

¹Easterly Scientific

²Y-12 National Security Complex

³Oak Ridge National Laboratory, Center for Radiation
Protection Knowledge

<https://ornl.gov/crpk>
crpk@ornl.gov

